energy&fuels

pubs.acs.org/EF Article

Ex Situ Catalytic Fast Pyrolysis of Lignin-Rich Digested Stillage over Na/ZSM-5, H/ZSM-5, and Fe/ZSM-5

Neil Priharto,* Stef Ghysels,* Mehmet Pala, Wim Opsomer, Frederik Ronsse,* Güray Yildiz, Hero Jan Heeres, Peter J. Deuss, and Wolter Prins*

Cite This: *Energy Fuels* 2020, 34, 12710−12723 Read Online

ACCESS | Metrics & More | Article Recommendations

ABSTRACT: The global increase in lignocellulosic ethanol production goes in tandem with an increase in lignin-rich stillage that remains underutilized to date. Anaerobic digestion could valorize residual (biodegradable) organic fractions into biogas, leaving a lignin-rich digested stillage (LRDS). This LRDS from the lignocellulosic ethanol production has been assessed as a feedstock for slow and fast pyrolysis in earlier studies, with the intention to increase the overall output of useful products or energy carriers from the starting material. While using this lignin-rich feedstock, *ex situ* catalytic vapor-phase upgrading (VPU) of fast pyrolysis vapors with fractional condensation was conducted over Na/ZSM-5, H/ZSM-5, and Fe/ZSM-5 catalysts. Semicontinuous fast pyrolysis experiments have been carried out at a reaction temperature of 480 °C in a mechanically stirred sand bed, which was connected directly to a fixed bed of catalyst particles for *ex situ* upgrading of the fast pyrolysis vapors. The carbon and mass yields in heavy phase liquids decreased after catalytic VPU (mass: *ca.* 8−11 wt %; carbon: *ca.* 11−15 wt %), compared to noncatalytic pyrolysis (mass: *ca.* 18 wt %; carbon: *ca.* 23 wt %). However, the yield in specific compounds, that is, alkylphenols and aromatics such as BTX, increased much upon catalytic VPU (especially for Fe/ZSM-5). For Fe/ZSM-5, the concentration in alkylphenols and aromatics was 20.8 wt % on liquid basis and the yield was 1.7 wt % on as-received (a.r.) feedstock basis. For noncatalytic pyrolysis, the concentration in alkylphenols and aromatics was 2.1 wt % (liquid basis) with a yield of 0.4 wt % (a.r. feedstock basis). This study thus demonstrates the potential of (modified) catalysts to upgrade lignin pyrolysis vapors.

1. INTRODUCTION

Lignin-rich digested stillage (LRDS) is a novel feedstock for pyrolytic valorization, derived from second-generation bioethanol production.[1,2] It is the solid residue obtained after alcoholic fermentation, followed by anaerobic digestion for biogas production. Conventional pretreatment and simultaneous saccharification and fermentation (SSF) do not seem to convert the entire cellulose fraction and disrupt the lignin structure significantly. This results in the build-up of unprocessed solid stillage. By consecutive anaerobic digestion, biodegradable holocellulose is valorized to biogas, while the less-biodegradable lignin can be valorized by means of pyrolysis (*i.e.*, at elevated temperature).

High-lignin feedstock materials, such as those derived from some bioethanol hydrolysis-based systems, have been subjected to fast pyrolysis.[3] Fast pyrolysis is a thermochemical conversion process which employs elevated temperatures (typically between 450 and 550 °C) with short hot vapor residence times (*ca.* 1−2 s) to thermally decompose the biomass feedstock in an oxygen-free environment.[4,5] During the fast pyrolysis process, the lignin-rich feedstock undergoes a number of thermally induced reactions simultaneously, for example, dehydration, depolymerization, aromatic ring cracking, and condensation reactions.[6] Previous work indicated that LRDS could be pyrolyzed successfully (because of the presence of residual carbohydrates) with staged condensation to produce separate heavy and aqueous pyrolysis liquids, in addition to biochar and noncondensable gases (NCGs).[2]

One of the anticipated drawbacks in fast pyrolysis of LRDS is the chemical instability of the produced pyrolysis liquids because of the presence of reactive aldehydes and phenolics that can undergo repolymerization.[7−9] The heavy phase of pyrolysis liquid also contains a large amount of high-molecular-weight compounds, in the form of dimers, trimers, and oligomeric phenols,[7,10] making the heavy pyrolysis liquid a waxy, highly viscous phase. These characteristics hinder the direct utilization of the heavy phase pyrolysis liquids for transportation fuel.[11,12]

Various methods have been tested to improve the quality of the heavy phase pyrolysis liquids, including for instance catalytic hydrotreatment, hydrocracking, catalytic esterification, and alkylation.[13−15] These catalytic methods could however only be carried out at elevated temperature and pressure (*ca.* 300−400 °C at 10−20 MPa), with hydrogen gas as a reactant.[13,16] Moreover, consecutive hydrogenation often leads to (cyclo)alkanes that find applications as a fuel

Received: July 22, 2020
Revised: September 13, 2020
Published: September 15, 2020

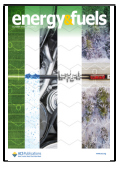

https://dx.doi.org/10.1021/acs.energyfuels.0c02390
Energy Fuels 2020, 34, 12710−12723

(additives). Although catalytic hydrotreatment of pyrolysis oil increases the yield in low-molecular-weight hydrocarbon compounds, the overall process also consumes quite some extra energy (pressure, hydrogen gas). Catalytic fast pyrolysis (CFP) does not require any additional energy and produces higher-quality pyrolysis liquids, compared to non-CFP, but in lower quantities.[17] There are two types of CFP, *in situ* CFP and *ex situ*, also known as vapor-phase upgrading (VPU).

During the *in situ* CFP, when the biomass is mixed into a bed of catalyst particles, pyrolysis vapors will be subjected to catalysis immediately after being generated and ejected from the biomass particle. Hence, catalytic reactions occur quickly after primary depolymerization. However, large catalyst-to-biomass ratios are typically required to ensure sufficient contact time between pyrolysis vapors and the catalyst. Other drawbacks associated with the *in situ* CFP is rapid catalyst deactivation due to the biomass-derived alkali and alkaline earth metals (*e.g.*, magnesium and potassium) that take part in ion-exchange reactions with protons at the catalyst's active surface,[18,19] along with coke accumulation on the catalyst particles (also holds true for *ex situ* CFP). For *in situ* CFP of lignin-rich biomass in particular, there is also the problem of bed agglomeration, which causes blockages and pressure drops and hampers the intimate biomass/catalyst contact. This bed agglomeration is due to lignin's tendency to melt and form char agglomerates encapsulating catalyst particles.[20,21] Biorefinery residues such as LRDS are however not pure lignin and may still contain non-negligible quantities of holocellulose, which in themselves may be beneficial to alleviate the melting and agglomeration behavior in fast pyrolysis to some extent.[3] However, problems related to low pyrolysis liquid yields and unfavorable liquid composition (high O content) remain.[2]

During catalytic VPU, pyrolysis vapors are swept over a catalyst bed at an elevated temperature of *ca.* 500 °C.[22−24] Catalytic VPU has the significant advantage that direct contact with biomass minerals is avoided and that primary pyrolysis is decoupled from VPU, allowing different reaction temperatures. Catalytic fixed bed VPU also prevents melting-lignin-induced catalyst agglomeration. There is no risk of vapors by-passing any catalyst agglomerates, as in *in situ* CFP.

One common type of catalysts that is being used in catalytic VPU are zeolite-based catalysts, specifically, ZSM-5. ZSM-5 is a conventional catalyst (additive) employed in the fluid catalytic cracking (FCC) of vacuum gas oil in petrochemical refineries. Zeolite catalysts have a low cost-to-yield ratio, are easily produced on a large scale, can be regenerated, and allow modifications to accommodate a specific reaction (*e.g.*, cracking and aromatization reaction). Zeolite catalysts can be impregnated with dopants (*e.g.*, Na/ZSM-5 and Fe/ZSM-5) to increase the reactivity/selectivity and enhance other reaction pathways.[23−26]

Although H/ZSM-5 catalysts mainly result in aromatic compounds from pyrolysis vapors of softwood Kraft lignin,[27] the presence of iron in ZSM-5 (Fe/ZSM-5) increases the selectivity to aromatics and the catalyst lifetime by reducing the acidity of the catalyst by weakening the Brønsted acid sites.[25,28] Next to ZSM-5, other zeolites (HY, MCM-41) have also been used as they feature a different porosity.[29]

Several publications are dealing with catalytic VPU of lignin in analytical pyrolysis (py-GC/MS), either analyzing multiple lignin sources or lignin cofeeding,[30−32] while screening or testing various VPU catalysts.[33] Nonanalytical pyrolysis studies (*i.e.*, employing bench- or lab-scale setups with condensation) are scarcer, especially for (semi) continuous catalytic VPU of lignin. This is partially due to the known difficulties (melting and agglomeration) of lignin pyrolysis in the first place.[3,34] Table 1 summarizes the results from bench-/lab-scale lignin pyrolysis with catalytic VPU.

A number of things can be learned from the literature studies listed in Table 1. First, full specifications of the used lignin are sometimes absent. Moreover, some basic characteristics of the used lignin have been omitted. For instance, the lignin used by Xie et al. presumably contained a significant fraction of residual carbohydrates,[36] evidenced by carbohydrate-derived furans and 2-cyclopenten-1-one in the pyrolysis liquids.[41] Second, the majority of studies performed batch pyrolysis on gram scale. Only one study was found to report catalytic VPU of lignin vapors at lab scale (66−108 g lignin per hour) using H/ZSM-5.[37] Third, in none of the studies in Table 1, a discrimination was made between aqueous liquids and heavy organic liquids. Moreover, a liquid analysis was often missing or specifically dedicated to specific (groups of) compounds.

This study therefore performed catalytic VPU of pyrolysis vapors from LRDS in a laboratory-scale mechanically stirred bed fast pyrolysis reactor (60 g per hour) to add value to the lignocellulosic ethanol production chain. The pyrolysis vapors were led over a catalyst bed of H/ZSM-5 and over Fe/ZSM-5 or Na/ZSM-5 to assess the effect of dopants. Sodium as a zeolite dopant has been shown to increase the yield in desired compounds in bio-oils (*i.e.*, aromatics and phenols).[42] Additionally, the partial ion exchange of Na^+ in ZSM-5 is believed to partially offset its acidity, which may be desirable, as pure H/ZSM-5 has shown a very large tendency for catalytic dehydration and coke formation in biomass pyrolysis.[43] Similarly, ion-exchanging H/ZSM-5 with potassium has shown to improve the deoxygenation activity while lowering the cracking activity yielding gases and coke.[44] On the other hand, Fe/ZSM-5 has shown a better selectivity toward monoaromatics rather than PAHs in comparison to unmodified H/ZSM-5.[45] Comprehensive liquid analysis was performed by means of elemental composition, GC × GC, gel permeation chromatography (GPC), and HSQC 2D NMR. The best performing catalyst is sought that results in the least complex (*i.e.*, containing a high fraction of low-molecular compounds), highly calorific liquids [*i.e.*, high higher heating value (HHV)], and rich in valuable compounds (*i.e.*, alkylphenolics) that are obtained at the highest yield.

2. MATERIALS AND METHODS

2.1. Lignin-Rich Digested Stillage. LRDS was obtained by ethanol fermentation of an acid-pretreated poplar coppice from Belgium at the Bio-based Europe's Pilot Plant (Ghent, Belgium), followed by anaerobic digestion in the Center for Microbial Ecology and Technology (CMET), Ghent University, as described by Ghysels et al.[1] Figure 1 shows the procedures performed to obtain the feedstock and the subsequent process in this study.

The original feedstock for the second-generation bioethanol production was a short-rotation poplar coppice, harvested in Lochristi (Belgium). The poplar coppice sample was chipped and sieved to *ca.* 1 cm and successively presteamed with bisulfite/sulfuric acid mixture (mass ratio of 4:1) at 170 °C for 30 min. A screw press and a filter press were used to recover the solids, which were water-washed before fermentation. The pretreated poplar was used for simultaneous SSF using ethanol yeast (Ethanol Red, Fermentis, France). The broth was distilled for bioethanol recovery, and the stillage was further processed via anaerobic digestion for biogas production. The anaerobic

https://dx.doi.org/10.1021/acs.energyfuels.0c02390
Energy Fuels 2020, 34, 12710−12723

Table 1. Overview of Literature on Fast Pyrolysis with Catalytic VPU of Lignin Vapors in Bench- and Lab-Scale Reactors

feedstock	VPU catalyst	reactor and operation	main observations	references
lignin (unspecified type)	Fe/ZSM-5	fixed bed batch reactor; 400−700 °C; 1 g per experiment	*ca.* 35−55 wt % liquids; no liquid compositional analysis	35
lignin (unspecified type)	Co/ZSM-5; ZSM-5	batch microwave reactor; 308−591 °C. Used quantity of feedstock not specified	*ca.* 18−24 wt % liquids; furans: *ca.* 16−23 area %; ketones: *ca.* 8−25 area % (mostly 2-cyclopenten-1-one and derivatives), and phenolics: *ca.* 12−23 area % (phenol and alkylphenols)	36
lignin residue from lignocellulosic ethanol from wheat straw (Inbicon, Denmark)	H/ZSM-5	continuous pyrolysis centrifuge reactor; 500 °C; hot vapor residence time of 1.8 s; 66−108 g h^{-1} feedstock throughput	*ca.* 3−9 wt % organic liquids (daf); 24.4−33.3 wt % total liquids; 21−24 wt % reaction water (daf); only oxygen-free volatiles reported: 1−4 wt % on feedstock basis (daf)	37
Kraft lignin	H/ZSM-5	fixed bed batch reactor; 3 g per experiment; 500−600 °C	*ca.* 30−35 wt % liquids; *ca.* 40 area % alkylphenols; *ca.* 20 area % guaiacols in liquids	38
wheat straw lignin from Lanxu Biotechnology	H/ZSM-5; HY; β-zeolite; MCM-41; ZnO/H/ZSM-5; ZnO/HY	benchtop batch pyrolysis; 500−750 °C; 3 g pyrolysis	*ca.* 10−30% carbon yield in liquids; ammonia used in gas phase to obtain aromatic amines; coproduction of phenol, alkylphenol, guaiacol, and aromatic hydrocarbons	29
pyrolytic lignin, alkali lignin, and Kraft lignin	H/ZSM-5; HY; β-zeolite; MCM-41; ZnO/H/ZSM-5; ZnO/HY	benchtop batch pyrolysis; 0.5 g per experiment; 500−800 °C	*ca.* 40−60 wt % liquids; high selectivity toward toluene and benzene	39
alkali lignin	H/ZSM-5	microwave fixed bed batch rector; 250−550 °C; used quantity of feedstock not specified	*ca.* 22−29 wt % liquids; *ca.* 30 area % alkylphenols; *ca.* 20 area % MAHs; *ca.* 25 area % PAHs	40

digestion was conducted in a 53 L stainless steel reactor at 35 °C for 30 days at an organic loading rate of 8 g COD l^{-1} day^{-1}.

The digestate, that is, the slurry obtained subsequently to the anaerobic digestion, was then dried and used for fast pyrolysis and catalytic VPU. The LRDS was received in a bulk dried form. The LRDS was milled and sieved until uniformly sized between 2 and 4 mm. Silica sand (PTB-Compaktuna, Gent, Belgium) with a particle density of 2650 kg m^{-3} and a mean diameter of 250 μm was used as the bed material in the mechanically stirred bed pyrolysis reactor.

ZSM-5 catalysts with three different dopant cations were used, *viz.*, H/ZSM-5, Na/ZSM-5, and the metal zeolite catalyst Fe/ZSM-5. H/ZSM-5 (50 wt % zeolite ZSM-5, 50 wt % alumina) was obtained after mixing alumina (Al_2O_3) powder Pural SB Catapal from Sasol (Hamburg, Germany), H/ZSM-5 powder CBV 2314 (SiO_2/Al_2O_3 = 23) from Zeolyst (Farmsum, The Netherlands), water, and an aqueous acid solution. A paste was obtained that was extruded as fine rods, which were crushed and sieved to obtain catalyst particles with a size between 1.0 and 3.0 mm. These were then subjected to calcination (16 h at 350 °C, followed by 16 h at 600 °C). The obtained extrudates had a BET surface area of 273 m^2/g and a micropore volume of 0.06 cm^3/g. Na/ZSM-5 was kindly provided by Zeochem AG (Rüti, Switzerland), specifically the type Zeocat Z-400 which came in 1.2−2 mm spherical granules and had a SiO_2/Al_2O_3 ratio of 400. The BET surface area of this catalyst was 280 m^2/g and the micropore volume was 0.02 cm^3/g.[46] The Fe/ZSM-5 catalyst was provided by Albemarle (Amsterdam, The Netherlands) and had a similar SiO_2/Al_2O_3 ratio as the first, H/ZSM-5 catalyst used in this study. This catalyst however was provided in a powder form (Geldart type B powder). Unfortunately, its full specification cannot be disclosed. Before use, all catalysts were calcined at 500 °C for 24 h.

2.2. Experimental Setup. Catalytic VPU experiments have been carried out in a lab-scale process unit involving a mechanically stirred bed reactor connected to a catalytic fixed bed reactor (Figure 2).

The experimental setup (stainless steel) allowed to measure the individual masses of liquid, solid, and gaseous products, thus enabling the calculation of mass balances of all product streams from fast pyrolysis and catalytic VPU. The bed diameter and height were 7 and 45 cm, respectively, while the above bed reactor void was 35 cm in height and 10 cm in diameter.[47] The reactor is equipped with a mechanical stirrer (4), providing bed content mixing, that is, quartz sand and LRDS. The nitrogen gas flow swept the primary pyrolysis vapors generated in the mechanically stirred bed over the catalyst bed (6) and subsequently to the condensation units. The nitrogen gas volumetric flow rate was controlled at approximately 180 L h^{-1} and was fed from the bottom of the reactor. A small fraction (*ca.* 5% total mass flow) of the nitrogen flow was fed from the top of the reactor to purge the top of the reactor and thus prevent vapors from accumulating and condensing on the top reactor walls. The LRDS was placed in a nitrogen-purged vibration-assisted lock hopper (3) and then fed into the feeding screw (2). Approximately 10 g of the LRDS was fed intermittently every 10 min to achieve a biomass feeding rate of *ca.* 60 g per hour. The overall vapor residence time of the pyrolytic vapors from devolatilization to condensation was approximately 60 s. These vapor-phase residence times are higher than what is normally expected in fast pyrolysis and thus could promote the secondary vapor-phase cracking reactions. This exact same setup was also used by Yildiz et al. running pine wood and the resulting pyrolysis liquids were benchmarked against reference, commercial pyrolysis liquids.[47] Even though the pyrolysis liquid yield was lower in the stirred bed reactor (52 wt %), the composition of the pyrolysis liquid was found to be in general, similar. The vapors that reach the catalyst bed will undergo extensive catalytic cracking; hence, extra thermal cracking associated with a slightly increased vapor residence time (5−10 s in the current setup) in the catalytic bed is deemed negligible. Small variations in the vapor residence time occurred because of the intermittent feeding regime creating a sinusoid-like pattern in the gas flow rate. All the experiments were performed in duplicate.

Thermocouples were installed in several parts of the reactor, enabling real-time monitoring of the reactor part temperature profile.

https://dx.doi.org/10.1021/acs.energyfuels.0c02390
Energy Fuels 2020, 34, 12710−12723

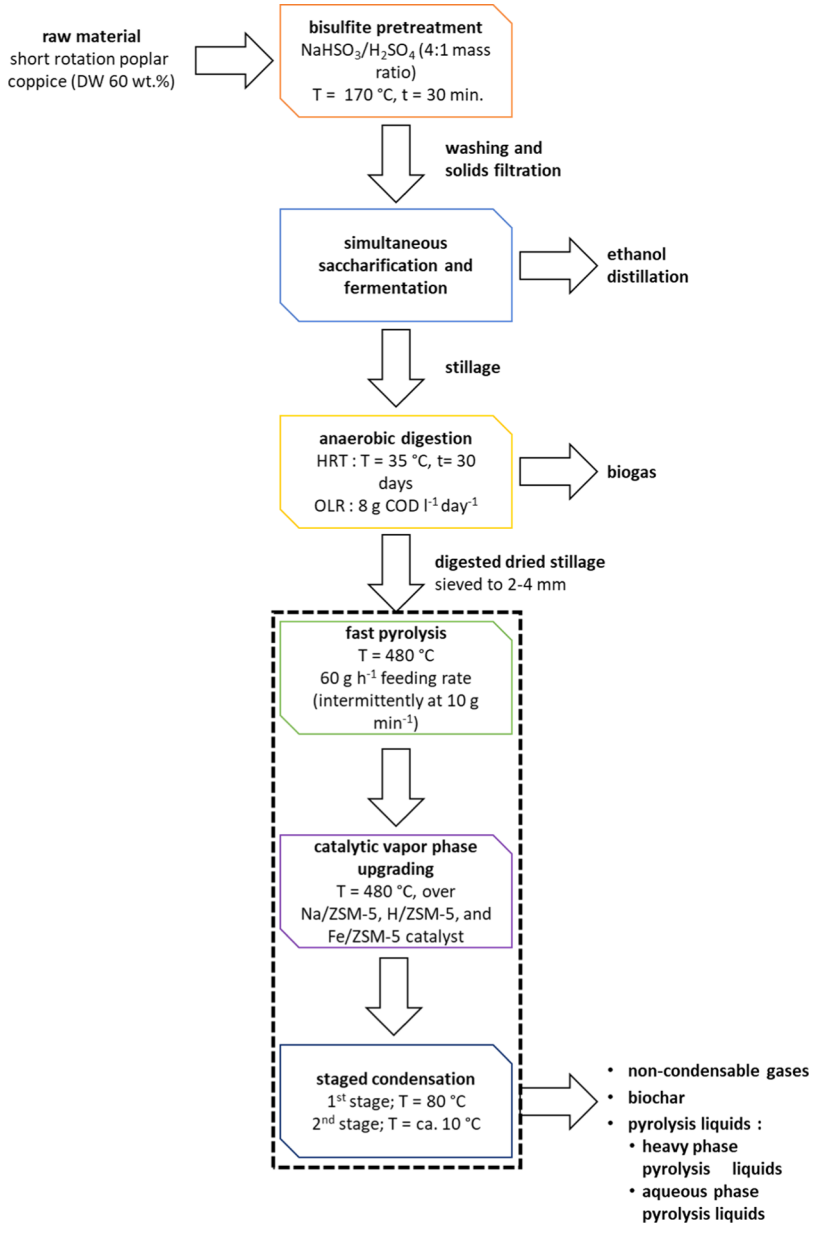

Figure 1. Block flow diagram of the feedstock production and catalytic VPU with staged condensation.

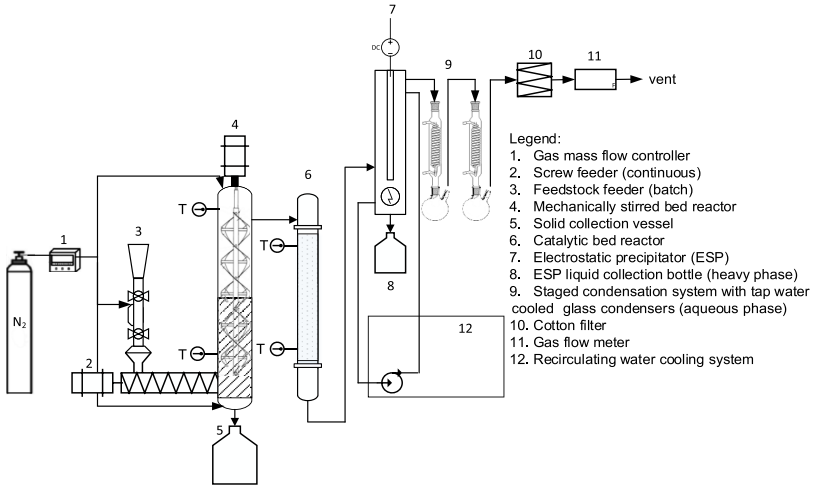

Figure 2. Scheme of the mechanically stirred bed reactor with an in-line catalytic bed for VPU.

https://dx.doi.org/10.1021/acs.energyfuels.0c02390
Energy Fuels 2020, 34, 12710−12723

Fast pyrolysis (with a knock-out vessel instead of a catalytic chamber) and catalytic VPU with the three different catalysts were conducted at 480 °C for both the mechanically stirred bed and the fixed bed. An earlier study by the authors concluded that 480 °C pyrolysis temperature resulted in the highest liquid yield using the LRDS feedstock.[2] Experimental parameters are summarized in Table 2.

Table 2. Experimental Parameters

parameters	value	unit
nitrogen volumetric flow rate	180	L h^{-1}
feeding rate[a]	60	g h^{-1}
feedstock size	0.2−0.4	cm
catalyst size	1.0−3.0	mm
ex situ catalyst mass	50	g
pyrolysis reactor temperature	480	°C
fixed catalyst bed temperature	480	°C

[a]Intermittently fed: 10 g for every 10 min.

Fractional condensation of catalytically upgraded pyrolytic vapors began in the electrostatic precipitator (ESP) (7). The ESP wall temperature was maintained at 80 °C, enabling the condensation of the heavier fraction of the vapors next to trapping aerosols. Further condensation of the remaining portion of vapors took place in two tap-water-cooled condensers (9) which were maintained at *ca.* 10 °C and connected in series. NCGs passed through a cotton filter (10) to remove the residual fine entrained solid particles and uncollected aerosols. The volumetric flow rate of exhaust gases was measured by a gas flow meter (11) (Gallus diaphragm gas meter, Itrón, Dordrecht, The Netherlands) before a sampling port for off-line GC analysis.

After each experiment, the heavy pyrolysis liquid phase was collected from the ESP collection flask, while the aqueous pyrolysis liquid phase was collected from the tap-water-cooled condenser flasks (two flasks). A small fraction of heavy pyrolysis liquid phase was found in the tap-water-cooled condenser flasks and vice versa; therefore, all pyrolysis liquids were filtered and separated. The spent catalysts were collected and put through loss-on-ignition (LOI) analyses to calculate the amount of coke formed during catalytic VPU. Inlet and outlet gas flow rates and temperature were also monitored during each experiment.

Yields in each fast pyrolysis and catalytic VPU product (heavy and aqueous phases of pyrolysis liquids, char, and NCG) were calculated in wt % relative to the feed on an as-received basis. Before and after each experiment, the mass of the catalyst bed, ESP ($m_{ESP,i}$ and $m_{ESP,f}$), the glass condenser flasks ($m_{cond,i}$ and $m_{cond,f}$), and the cotton filter ($m_{filter,i}$ and $m_{filter,f}$) (including the piping) were weighed. The subscripts i and f denoted initial and final, respectively.

2.3. Products and Yield Calculations. The heavy phase yield (Y_{heavy}) was calculated from the mass difference in ESP and the cotton filter, added with a small amount of heavy pyrolysis liquid phase in both tap-water condenser flasks ($m_{h,aq}$), subtracted by the amount of aqueous phase in the ESP ($m_{aq,h}$), and the result is divided by the feedstock mass (m_f) as shown in eq 1.

$$Y_{heavy} = [(m_{ESP,f} - m_{ESP,i}) + (m_{filter,f} - m_{filter,i}) + m_{h,aq} - m_{aq,h}] \times \frac{100}{m_f} \quad (1)$$

The aqueous phase yield (Y_{aq}) calculation was based on the mass difference in both glass condenser flasks while also adding the amount of aqueous phase in the ESP ($m_{aq,h}$) divided by the feedstock mass (m_f), as shown in eq 2.

$$Y_{aq} = ((m_{cond1,f} - m_{cond1,i}) + (m_{cond2,f} - m_{cond2,i}) + m_{aq,h} - m_{h,aq}) \times \frac{100}{m_f} \quad (2)$$

Char yield calculation (Y_c) was determined by subjecting the collected solids (char and bed material) to LOI analysis, which refers to the mass loss of a sample after ignition and combustion (Δm_{loi}). The LOI analysis was carried out in a muffle furnace (Carbolite AAF 1100) at 600 °C for a minimum of 6 h. Char yield is calculated based on the loss-of-mass (Δm_{loi}) of collected solids (char and bed material) after LOI analysis and compensated for the ash content (A_c) (in wt %). The total char yield was the summation of loss-of-mass value, added by char in the heavy phase pyrolysis liquids ($m_{c,h}$) obtained by filtering and corrected for the char sample mass that was taken for analysis ($m_{c,rm}$) as given in eq 3.

$$Y_c = \left[\left(\frac{\Delta m_{loi}}{100\% - A_c}\right) + m_{c,h} + m_{c,rm}\right] \times \frac{100}{m_f} \quad (3)$$

The NCG yield (Y_{NCG}) (eq 4) was calculated based on the mass difference between the average volumetric gas flow rate during feedstock feeding ($\overline{Q_s}$) at the outlet and the average baseline volumetric gas rate flow (nitrogen) ($\overline{Q_b}$) for the duration of each experiment (t). Conversion of volumetric gas flow rates to mass flow rates was done by determining the mixture gas density. Considering the nonideal nature of pyrolytic NCG, mixture gas densities (ρ_{NCG}) were calculated using the Peng−Robinson equation of state based on NCG composition (N_2 free) as analyzed by the micro-GC and on the temperature and pressure of the outlet gas.

$$Y_{NCG} = [(\overline{Q_s} - \overline{Q_b}) \cdot t \cdot \rho_{NCG}] \times \frac{100}{m_f} \quad (4)$$

As a direct consequence of mass balance fundamentals, mass balance closure is defined as the sum of both pyrolytic liquid yields, char yield, and NCG yield (eq 5).

$$Y_{tot} = Y_{heavy} + Y_{aq} + Y_c + Y_{NCG} \quad (5)$$

2.4. Analytical Techniques. *2.4.1. Energy Content.* The energy content of the feedstock, char, and heavy phase pyrolysis liquids was calculated from their elemental compositions using the Milne equation.[48] The energy content of NCGs was derived with Aspen Hysys (AspenTech, Bedford, USA) using the gas composition and temperature of the gas outlet. Aspen Hysys calculates the HHV of NCG based on the gas correlation methods and data from ISO 6976:1995 (calculation of calorific values, density, relative density, and Wobbe index from the composition).

2.4.2. Moisture, Ash, and Lignin Content. The quantification of moisture and ash in LRDS were, respectively, conducted following ASTM E871-82 (standard test method for moisture analysis of particulate wood fuels) and ASTM E1755-01 (standard test method for ash determination in biomass). Acid-insoluble lignin fraction was determined according to the Technical Association of the Pulp and Paper Industry (TAPPI) T222 om-02 (Acid-insoluble lignin in wood and pulp test) method by the Department of Plant Systems Biology, Flanders Institute of Biotechnology, Belgium. Pyrolytic solid content (*i.e.*, entrained fine char particles) in pyrolysis liquids was determined using filtration according to the ASTM D7579-09 (standard test method for pyrolytic solid content in pyrolytic liquids by filtration of solids in methanol). The char inside the mechanically stirred bed reactor has a high tendency to agglomerate with the inert quartz sand and could not be separated from the bed material. Therefore, the ash content of the chars (A_c) had to be determined by calculation. This was done through eq 6, based on the mass fraction accounted for by the elemental composition [carbon (ω_C), hydrogen (ω_H), nitrogen (ω_N), sulfur (ω_S), and oxygen (ω_O) all in wt % as received (a.r.)] from a small sample of pure char.

$$A_c = 100 - (\omega_C + \omega_H + \omega_N + \omega_S + \omega_O) \quad (6)$$

2.4.3. Elemental Composition. The elemental composition of the LRDS, chars, and heavy phase pyrolysis liquids was determined by using a FLASH 2000 organic elemental analyzer (Thermo Fisher Scientific, Waltham, USA) in CHNS and oxygen configuration. The instrument was equipped with a thermal conductivity detector

https://dx.doi.org/10.1021/acs.energyfuels.0c02390
Energy Fuels 2020, 34, 12710−12723

Table 3. LRDS Feedstock Characterization: Moisture Content (in wt % a.r.), Ash Content (in wt % a.r.), Elemental Composition (in wt % a.r.), HHV (in MJ kg^{-1} a.r.), and Klason Lignin (in wt % d.b.)

		elemental composition					
moisture content	ash content	C	H	N	O	HHV	Klason lignin
5.7 ± 0.2	10 ± 0.1	50.2 ± 0.8	5.5 ± 0.0	2.7 ± 0.1	26.4 ± 1.5	20.6 ± 0.1	63.2 ± 0.7

Table 4. Comparison of CFP Product Yields in the Presence of ZSM-5-Based Catalysts (wt % on Feed Basis a.r.)

	yield			
products	Na/ZSM-5	H/ZSM5	Fe/ZSM-5	non-catalytic
heavy phase	10.92 ± 3.20	9.80 ± 0.86	7.94 ± 0.66	18.08 ± 2.62
aqueous phase	10.04 ± 0.33	11.86 ± 0.49	11.94 ± 1.49	9.86 ± 2.62
char	39.65 ± 1.08	40.31 ± 0.82	39.76 ± 1.81	39.47 ± 2.76
NCG	43.42 ± 0.08	36.43 ± 0.47	33.68 ± 1.67	28.23 ± 2.10
coke	0.9 ± 0.15	0.99 ± 0.09	0.46 ± 0.0	
total[a]	104.03 ± 3.39	97.90 ± 1.37	93.32 ± 2.95	97.10 ± 5.08

[a]Excluding coke in the catalyst bed.

(TCD). 2,5-(Bis(5-*tert*-butyl-2-benzo-oxazol-2-yl) thiophene (for CHNS detection configuration) and methionine (for oxygen detection configuration) were used as standards. High-purity helium (Alphagaz 1, purity ≥ 99.995%, Air Liquide, Belgium) was used as a carrier gas and reference gas. High-purity oxygen (Alphagaz 1, purity ≥ 99.995%, Air Liquide, Belgium) was used as the combustion gas.

2.4.4. NCG Analyses. The composition of the produced pyrolytic NCGs was determined off-line using an 490 Micro GC from Agilent Technologies using a 5 mL gastight syringe. The micro GC is equipped with two analytical columns with TCDs. The first column (10 m Molesieve 5 Å with backflush) operated at 75 °C to separate H_2, N_2, CH_4, and CO, while the second column (10 m PPU) operated at 70 °C and used for the separation of CO_2, C_2H_4, C_2H_6, C_3H_6, and C_3H_8. High-purity helium (Alphagaz 1 from Air Liquide) was used as the carrier gas.

2.4.5. Ash Composition Analysis. The ash compositions of the LRDS were identified and measured using inductively coupled plasma optical emission spectrometry (ICP-OES). The analysis was performed using methods described in Yin et al.[49] ICP-OES was performed on a PerkinElmer 7000DV. Prior to analyses, the samples were sealed and then heated in a microwave oven to 200 °C in 10 min and then held at that set temperature for 15 min. The solid sample (20 mg) was added to an aqueous solution of HNO_3 (8 mL, 65 wt %, Sigma Aldrich). Subsequently, HNO_3 solution (2 wt % in water) was added to the sample up to a total volume of 50 mL. The resulting solution was diluted 10 times with deionized water.

2.4.6. Molecular Weight Distribution of the Heavy Phase Pyrolysis Liquids. The molecular weight distribution of the heavy phase pyrolysis liquids components was determined by GPC. GPC was performed using an HP1100 equipped with three 300 × 7.5 mm PLgel 3 μm MIXED-E columns in series using a GBC LC1240 RI detector. The average molecular weight calculations were performed with the PSS WinGPC Unity software from Polymer Standards Service (Amherst, MA, USA). Tetrahydrofuran (THF) was used as the eluent at a flow rate of 1 mL min^{-1}, and toluene was used as a flow marker. The column pressure was set at 14 MPa and a temperature of 42 °C. Approximately 20 μL of the sample was injected into the column at 10 mg mL^{-1} sample concentration.

2.4.7. Analyses for the Heavy Phase Pyrolysis Liquids. The composition of the heavy phase pyrolysis liquids was analyzed using two different techniques: dual-axis gas chromatography with a flame ionization detector (GC × GC-FID) and two-dimensional (^1H and ^{13}C) heteronuclear single-quantum coherence nuclear magnetic resonance (2D HSQC-NMR) spectroscopy. GC × GC-FID analyses were performed using methods described by Kloekhorst et al. and Wildschut et al.[13,50] The GC × GC-FID from Interscience is equipped with a cryogenic trap system and two columns: a 30 m × 0.25 mm i.d. and 0.25 μm film thickness Restek RTX-1701 capillary column connected by a meltfit to a 1.20 m × 0.15 mm i.d. and 0.15 μm film thickness Restek Rxi-5Sil MS column. The GC × GC with FID was also coupled with a dual-jet modulator using liquid carbon dioxide to trap the samples, using a modulation time of 6 s. The carrier gas was helium (Alphagaz-1 from Air Liquide), and the flow was continuously controlled at 0.6 mL min^{-1}. The injector pressure was set at 70 kPa, while the temperature and FID temperature were set at 250 °C. The oven temperature was initially set at 40 °C for 5 min and then ramped up to 250 °C at a rate of 3 °C min^{-1}.

The FID-response plot was analyzed using GC Image software (GC Image, Lincoln, US). The identification of the primary component groups (*e.g.*, alkanes, aromatics, and alkylphenolics) in the pyrolysis liquids were made by injecting representative model compounds from each component group. Quantification of the component groups was performed by using the average relative response factor of compounds in each group. *n*-Dibutyl ether (DBE) was used as an internal standard. Before GC × GC-FID analyses, the samples were diluted with equal volume of THF (*i.e.*, 50 wt % sample in THF) and DBE was added at a final concentration of 1000 ppm.

Two-dimensional ($^1H-^{13}C$) HSQC-NMR analyses were also conducted using methods described by Lancefield et al.[51] NMR was performed using a Bruker Ascend 700 and 500 MHz spectrometers equipped with CPP TCI and CPP BBO probes, respectively. In each analysis, approximately 0.1 g of heavy phase pyrolysis liquid samples was dissolved in 1 g of dimethyl sulfoxide (DMSO)-d_6. Semi-quantitative 2D HSQC NMR analysis was performed using MestReNova version 11.0 (Mestrelab Research, Santiago de Compostela, Spain).

3. RESULTS AND DISCUSSION

3.1. Feedstock Characteristics. The LRDS characteristics are summarized in Table 3. The LRDS largely consisted of acid-insoluble lignin (63.2 wt %), and, to a smaller extent, residual holocellulose and microbial biomass (as evidenced by the high N-content). The initial ash within the poplar coppice concentrated in the LRDS during the bioethanol and biogas production processes, explaining the high ash mass fraction in LRDS. Before pyrolysis, the moisture content of the LRDS was reduced to 5.7 wt %, as the water in the feedstock will further dilute the aqueous phase obtained in the pyrolysis liquids. Elemental analysis also shows that half of the feedstock is carbon (by mass). The high carbon content contributes to the energy content of the feedstock itself. Compared to other lignin-rich streams, for example, residue from ethanol production by two-stage weak acid hydrolysis of softwood (ETEK lignin) and organosolv alcell lignin, LRDS has almost the same carbon and energy content.[3,16]

https://dx.doi.org/10.1021/acs.energyfuels.0c02390
Energy Fuels 2020, 34, 12710−12723

3.2. Product Yields from Catalytic VPU of Lignin Vapors. The product yields of catalytic VPU over H/ZSM-5, Na/ZSM-5, and Fe/ZSM-5 catalysts are summarized in Table 4. The results of non-CFP of the same feedstock was used as a benchmark. For all experiments, satisfying mass balance closures (*ca.* 93−104%) and reproducibility (*i.e.*, low standard deviations in mass balance closures) were established. The yields in NCGs increased significantly upon *ex situ* VPU (33.7−43.4 wt %), compared to non-CFP (*ca.* 28.2 wt %). Coke was also formed in catalytic VPU (Table 4). Both this coke formation and the increased NCG production in catalytic pyrolysis occurred at the expense of heavy liquids that contain the products of interest (here, monoaromatic compounds). The amount of aqueous phase and char (the term is used to represent the solid residue that remained after pyrolysis) remained similar across all experiments. The ash concentration in the char was also similar in all types of catalysts, at approximately 21 wt % as produced. This high ash concentration in the char stems from the initial 10 wt % ash concentration in the feedstock and also explains why such (up to 40 wt % on feedstock basis) high char yields were obtained.

Figure 3 plots the mass yield in the heavy phase versus the carbon yield in the heavy phase. This also shows that, besides the mass yield, the carbon yield in heavy liquids for noncatalytic pyrolysis was the highest (23.3 ± 3.4 wt %). This loss in carbon in the heavy phases was due to the formation of NCGs and coke. Despite the lower mass and carbon yields in the heavy phases after catalytic VPU (compared to noncatalytic pyrolysis), the composition of the heavy phases upon catalytic VPU did change favorably (*vide infra*).

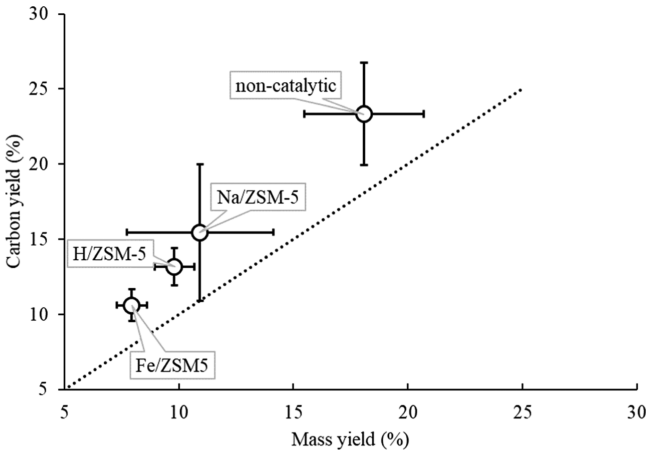

Figure 3. Mass yield vs carbon yield in the heavy phase liquids after noncatalytic pyrolysis and fast pyrolysis of LRDS with catalytic VPU.

Because of the novelty of this particular LRDS, direct comparison with other studies was difficult. Zhou et al. however used a comparable type of lignin from lignocellulosic ethanol production to perform pyrolysis at a comparable scale as this study (Table 1).[37] In their study, they obtained a total liquid yield of 45 wt % (daf) and a char yield of 29.2 wt % (daf) for noncatalytic pyrolysis, while the herein reported results for noncatalytic pyrolysis (Table 4, last column) show a lower total liquid yield of 27.44 wt % and higher char yield of 39.47 wt %. The higher char yield at the expense of the liquid yield is attributed to the elevated Klason lignin content of the LRDS (63.2%), compared to the lignin from wheat straw ethanol production (56.3% in Zhou et al.[37]). Indeed, high lignin contents are associated with higher tendencies to char formation rather than the production of condensables.[1] While using H/ZSM-5 catalyst at 500 °C, Zhou et al. observed less liquids (27.9 wt %, daf), a trend which is in line with this study.[37] A total liquid yield value *ca.* 24−26 wt % (daf) was calculated from Tables 3 and 4 (1.19 g LRDS (daf) corresponds to 1 g LRDS a.r.). Compared to the other studies in Table 1, the observed total liquid yields of this work are on the lower side, but those literature studies applied small bench-scale reactors in which vapor residence times were much shorter than in the current lab-scale system (see Section 2.2). This obscures a direct comparison.

The feedstock initially dries and devolatilizes to form primary pyrolysis vapors, which undergo consecutive thermal cracking and catalytic cracking in the presence of ZSM-5 catalysts. This variety of catalytic cracking reactions includes dehydration, decarboxylation, decarbonylation, Diels−Alder condensation, and aromatization, which eventually result in the production of aromatics and hydrocarbons.[17,21,52] Regarding water in the aqueous phase, it can be calculated that *ca.* 60% of that aqueous phase consisted of feedstock-derived water, assuming that all moisture (5.7 wt %) ended up on the aqueous phase upon condensation.

The increase of NCG at the expense of pyrolysis liquids suggests that all ZSM-5 catalysts promote further secondary cracking and reforming reactions. ZSM-5 catalysts were not involved in the initial devolatilization process; therefore, the char yield was similar to that of the non-CFP. Secondary cracking and repolymerization of lignin derivatives produced coke. This is deposited on the catalyst surface and will eventually block the catalyst pores, effectively rendering them inactive. Other reasons for catalyst deactivation are the removal of aluminum support from the catalyst due to water vapor (hydrothermal deactivation),[25] and the accumulation of inorganic contaminants on the surface of the catalyst swept along with the gas stream. Yet, the latter is minimal for *in situ* VPU.

Table 5 shows that catalytically produced heavy phases contain slightly more carbon and less oxygen (in oxygenated

Table 5. Elemental Analysis and Energy Content of the Heavy Phase Pyrolysis Liquids (wt % As Produced)

	Na/ZSM-5	H/ZSM-5	Fe/ZSM5	non-catalytic
nitrogen	5.51 ± 0.22	5.23 ± 0.3	6.31 ± 0.57	4.52 ± 0.09
carbon	71.07 ± 0.83	67.54 ± 1.74	67.15 ± 3.55	64.81 ± 0.64
hydrogen	7.57 ± 0.14	7.67 ± 0.22	7.6 ± 0.41	7.74 ± 0.06
sulfur	0.3 ± 0.03	0.15 ± 0.02	n.d.	n.d.
oxygen	15.34 ± 0.31	16.69 ± 0.05	16.81 ± 0.72	17.39 ± 0.28
HHV	31.7	30.6	30.2	27.2

https://dx.doi.org/10.1021/acs.energyfuels.0c02390
Energy Fuels 2020, 34, 12710−12723

compounds) than the noncatalytic heavy phase. The nitrogen content did not decrease upon catalytic VPU, in contrast to the oxygen content, which indicates that all ZSM-5 catalysts were more prone to deoxygenation rather than to denitrogenation. Hence, nitrogen accumulated in the heavy phases from catalytic VPU. ZSM-5 catalysts in general have a high selectivity toward aromatization reactions from pyrolysis vapors because of their pore size, steric hindrance, large pore volume, and high Brønsted acid site density.[17,21,25,52] Mutual differences among the different dopants are modest, but the following differences were observed from Table 5 and the van Krevelen diagram in Figure 4. The heavy phase from VPU with

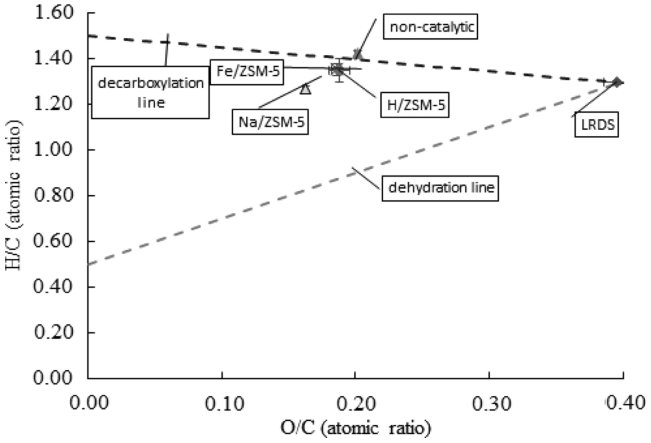

Figure 4. van Krevelen diagram of catalytic and noncatalytic pyrolysis liquids (heavy phase).

Na/ZSM-5 shows the highest carbon and lowest oxygen content compared to Fe/ZSM-5 and H/ZSM-5. Hydrogen and iron-doped ZSM-5 gave similar results in the carbon and oxygen content of the produced pyrolysis liquids, implying that both catalysts might have similar selectivity to deoxygenation reactions.

Starting from the feedstock, all heavy liquid phases followed a decarboxylation line upon catalytic pyrolysis of LRDS with different VPU catalysts. This trend is more pronounced for Na/ZSM-5, followed by both Fe/ZSM-5 and H/ZSM-5 and noncatalytic pyrolysis. This implies that net oxygen removal from the feedstock was rather in the form of CO_2 than in the form of water. The majority of water in the aqueous phase was feedstock-derived moisture (*vide infra*). Although the contribution of carbon dioxide in the NCGs was similar among pyrolysis experiments (Table 6), the yield in NCGs was the largest for Na/ZSM-5, followed by both Fe/ZSM-5 and H/ZSM-5 and noncatalytic pyrolysis, which is in accordance with the decarboxylation trajectory in the van Krevelen plot (Figure 4). In contrast, ethene and propene/propylene in the NCGs increased upon VPU, which is observed in Zhou et al. as well.[37] It should be noted that energy recovery from the NCGs is opportune, given the high CO and CH_4 (and H_2 in the case of Fe/ZSM-5) content.

3.3. Heavy Phase Catalytic VPU Liquid Characteristics. Regarding the product distribution, the main result of VPU is a conversion of heavy phase liquids to NCG and coke. It is now important to see if this loss of liquids (Figure 3) is balanced by an increase in the liquid quality, in a sense of chemical composition.

Figure 5 shows the GC × GC-FID chromatogram of heavy pyrolysis liquids produced over different ZSM-5 catalysts with a division of the 2D chromatogram into regions according to chemical functionalities. Region 1 is mainly cyclic alkanes; region 2 is primarily linear/branched alkanes; regions 3 and 4 are aromatics (4a are naphtalenes and 4b are polycyclic aromatic hydrocarbons); regions 5 and 6 are ketones, alcohols, and acids; and regions 7, 8, and 9 are phenols and phenolic compounds (including alkylphenolics and catechols). Also, "a" is the internal standard (DBE) and "b" is butylated hydroxytoluene (a stabilizer in THF).

The GC × GC-FID analysis shows that all heavy phase pyrolysis liquids from catalytic VPU exhibit different chemical compositions compared to the noncatalytic pyrolysis liquids (Figure 5 and Table 7).

All upgraded pyrolysis liquids contain a significant number of monoaromatic compounds (*e.g.*, benzenes, toluene, and xylene) and naphthalene. This confirms that cation-modified ZSM-5-enhanced deoxygenation reactions produce aromatic hydrocarbons. The result was in-line with various other studies employing H/ZSM-5 and metal-modified ZSM-5 catalysts.[37,39,40,53] Xie et al. reported significant quantities of furans and 2-cyclopenten-1-one derivatives,[36] but this was likely due to the holocellulose residues present in lignin.[41] It is also observed that the number of low-molecular-weight ketones decreased in the presence of a catalyst. Light oxygenates, such as esters, carboxylic acids, and alcohols, could be further cracked into NCGs (mainly CO_2 and, to a lesser extent, CH_4) through decarboxylation.[53] The alkylphenolic fraction was increased significantly upon catalytic VPU, seemingly at the expense of the phenolics fraction (Table 7). This can be due to phenols that have been alkylated in the presence of catalysts with the olefins present in the so-called hydrocarbon pool (formed mostly from the carbohydrate fraction).[54] Secondary alcohols can also act as alkylating agents.

It was calculated that only 16.1 wt % of the noncatalytic heavy pyrolysis liquid phase was volatile. The volatile mass fractions of the catalyzed pyrolysis liquids (GC detectable fraction) increased by *ca.* 30 to 100% (to a mass fraction of 21.6 to 33.1 wt % vs 16.1 wt % on heavy liquid phase basis) compared to the non-CFP liquids. This indicates a higher

Table 6. Composition of NCGs (Vol %) for Non-CFP and CFP with VPU

	H/ZSM-5 (%)	Fe/ZSM-5 (%)	Na/ZSM-5 (%)	noncatalytic (%)
hydrogen	0.3 ± 0.0	16.9 ± 2.2	0.2 ± 0.0	1.7 ± 0.2
methane	13.1 ± 1.1	12.8 ± 1.4	14.3 ± 0.5	15.6 ± 1.6
carbon monoxide	28.9 ± 1.4	20.3 ± 1.7	31.0 ± 3.5	25.0 ± 0.8
carbon dioxide	50.9 ± 1.0	49.5 ± 5.4	56.9 ± 4.2	55.8 ± 1.5
ethene	3.1 ± 1.3	0.3 ± 0.1	1.6 ± 0.2	1.2 ± 0.1
ethane	0.8 ± 0.2	0.8 ± 0.2	0.6 ± 0.1	0.8 ± 0.2
propene/propane	3.3 ± 1.1	0.6 ± 0.2	2.0 ± 0.1	1.3 ± 0.2

https://dx.doi.org/10.1021/acs.energyfuels.0c02390
Energy Fuels 2020, 34, 12710−12723

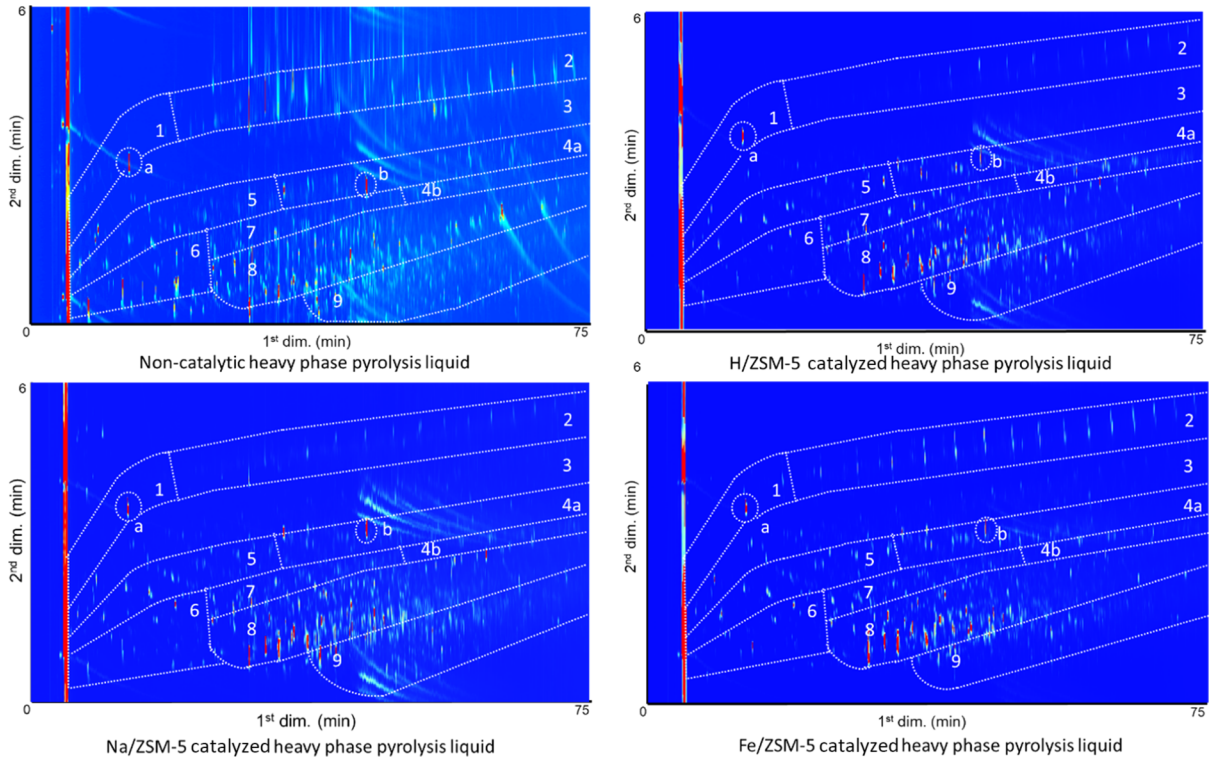

Figure 5. Results of GC × GC-FID analyses of catalytic and noncatalytic heavy phase fast pyrolysis liquids of LRDS.

Table 7. GC × GC-FID Quantification of Chemical Groups Found in Heavy Phase Catalytic and Noncatalytic Pyrolysis Liquids[a]

	Na/ZSM-5		H/ZSM-5		Fe/ZSM-5		non-catalytic	
group type	ω	Y	ω	Y	ω	Y	ω	Y
aromatics	2.3	0.3	3.1	0.3	4.9	0.4	0.6	0.1
cycloalkanes	0.2	0	0.9	0.1	2.3	0.2	0.1	0
catechols	1.1	0.1	1.3	0.1	0.7	0.1	2.3	0.4
alkanes	0.6	0.1	0.6	0.1	2.2	0.2	1.4	0.3
ketones, acids, and alcohols	2.4	0.3	2.2	0.2	3.4	0.3	4.0	0.7
alkylphenols	12.3	1.3	12	1.2	15.9	1.3	1.5	0.3
naphthalenes	2.0	0.2	2.7	0.3	2.8	0.2	0.5	0.1
phenolics	2.7	0.3	3.2	0.3	3.6	0.3	5.6	1.0
volatile fraction	23.6	2.6	26.0	2.6	35.8	3.0	16.1	2.9

[a]Concentration (ω) of these compounds is expressed in wt % in the heavy phase liquid and yield (Y) is expressed in wt % on LRDS feedstock basis.

degree of depolymerization to useful chemical compounds as a result of the VPU.

While CFP with VPU decreased the yield in heavy pyrolysis liquids remarkably, their volatile fraction increased drastically. This led to the observation that the yield in the volatile fraction on a.r. feedstock basis remained rather constant. The specific advantage of VPU, compared to non-CFP is that the volatile fraction becomes much simpler in composition, having only a few high-concentration compounds. Indeed, alkylphenols presented *ca.* 50% of the volatile fraction in the heavy phase from VPU. Non-CFP liquids were much more complex in composition and contained more low-concentration compounds. Phenolics constituted the largest group (by mass) in the heavy phase from noncatalytic pyrolysis but covered only *ca.* 35% of the volatile fraction.

Overall, *ca.* 4 times more alkylphenols were obtained through VPU, compared to noncatalytic pyrolysis of the same mass of starting material (Table 7). These alkylphenols, like cresols and xylenols, hold a certain value as these are chemical intermediates[55] and as a fuel (additives). The pool of unseparated alkylphenols, called cresylic acid, is also a useful outgoing product from fast pyrolysis of LRDS with VPU. Hence, the lower mass and carbon yields in the heavy liquids after VPU (Figure 3) are well compensated by the favorable composition of the upgraded heavy liquids.

The volatile fractions of the heavy phase can be correlated with its molar mass distribution (Figure 6). Quantitative GPC analyses results were not absolute and therefore only served as an estimate; all the GPC data were compared with polystyrene as a standard. Pyrolysis liquids from Fe/ZSM-5 catalysis have a narrow molar mass distribution with a single distinct peak at *ca.* 140 g mol^{-1}, suggesting an alkylphenol group or methylnaphthalene. Pyrolysis liquids from H/ZSM-5 and Na/ZSM-5 catalysis have a wider molar mass distribution with an additional peak at *ca.* 205 g mol^{-1} (C_{10}−C_{15} compounds). The distribution pattern indicates that the

https://dx.doi.org/10.1021/acs.energyfuels.0c02390
Energy Fuels 2020, 34, 12710−12723

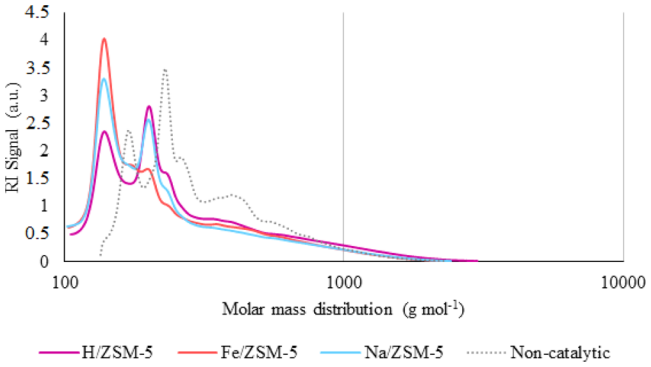

Figure 6. Gel permeation chromatogram comparison of heavy phase pyrolysis liquids produced by different catalysts.

degree of lignin depolymerization reactions in Fe/ZSM-5 was higher than in H/ZSM-5- and Na/ZSM-5-catalyzed pyrolysis liquids. This corresponds to the data presented in Table 7. The highest volatile fraction (33.1 wt %) was obtained with Fe/ZSM-5 being used as a catalyst. Lower volatile fractions were obtained for H/ZSM-5 and Na/ZSM-5, and the lowest for non-CFP. Generally, the lignin fraction of the feedstock was thermally decomposed during the initial devolatilization reactions, and the phenolic dimers (*ca.* 432 Da) in the vapors were subsequently cracked in the presence of cation-modified ZSM-5 catalyst.

The distinct GPC for heavy liquids from Fe/ZSM-5 catalysis suggests that the addition of iron to the catalyst structure impacted the chemical pathways of the decomposition of the used feedstock, thus affecting the molecular weight distribution and the composition of the heavy phase pyrolysis liquids. The Fe/H/ZSM-5 catalyst favored the formation of benzene and naphthalene and inhibited the production of *p*-xylene, ethylbenzene, and trimethylbenzene in comparison to unmodified H/ZSM-5.[56,56] Fe/H/ZSM-5 can promote the addition of benzene rings, resulting in the formation of a more considerable amount of naphthalene and its derivative. This suggests that the presence of Fe cations helps the aromatization of primary products to naphthalenes rather than the alkylation of initially formed benzene.[53,57,58]

Another difference regarding the composition of heavy liquids from VPU is that Fe/ZSM-5 tends to have a higher affinity toward alkanes and cycloalkanes. These (cyclo)alkanes in heavy liquids from Fe/ZSM-5 catalysis constituted 4.5 wt % (liq. basis) of the volatile fraction, while the same compounds only amounted to 0.4 wt % (liq. basis).

A more detailed map of the chemical composition of the heavy phase pyrolysis liquids was obtained using the 2D HSQC NMR analysis (Figure 7). The non-CFP heavy phase still contains a notable oscillating signal that corresponds with pyrolytic sugars (and sugar derivatives), phenolics, aliphatics, and aliphatic−aromatic groups. The pyrolytic sugars were produced from fast pyrolysis of minor residual cellulose and hemicellulose fractions, which (as stated earlier) were presumably still present in the LRDS and diminished after catalytic VPU over all the ZSM-5 catalysts. A tiny residue of pyrolytic sugars was still observed in the heavy phase pyrolysis liquids produced using Fe/ZSM-5 and Na/ZSM-5 catalysts. However, almost complete elimination of pyrolytic sugars was observed in H/ZSM-5 catalyst. The 2D HSQC NMR analyses also confirm the above-mentioned analysis results that only

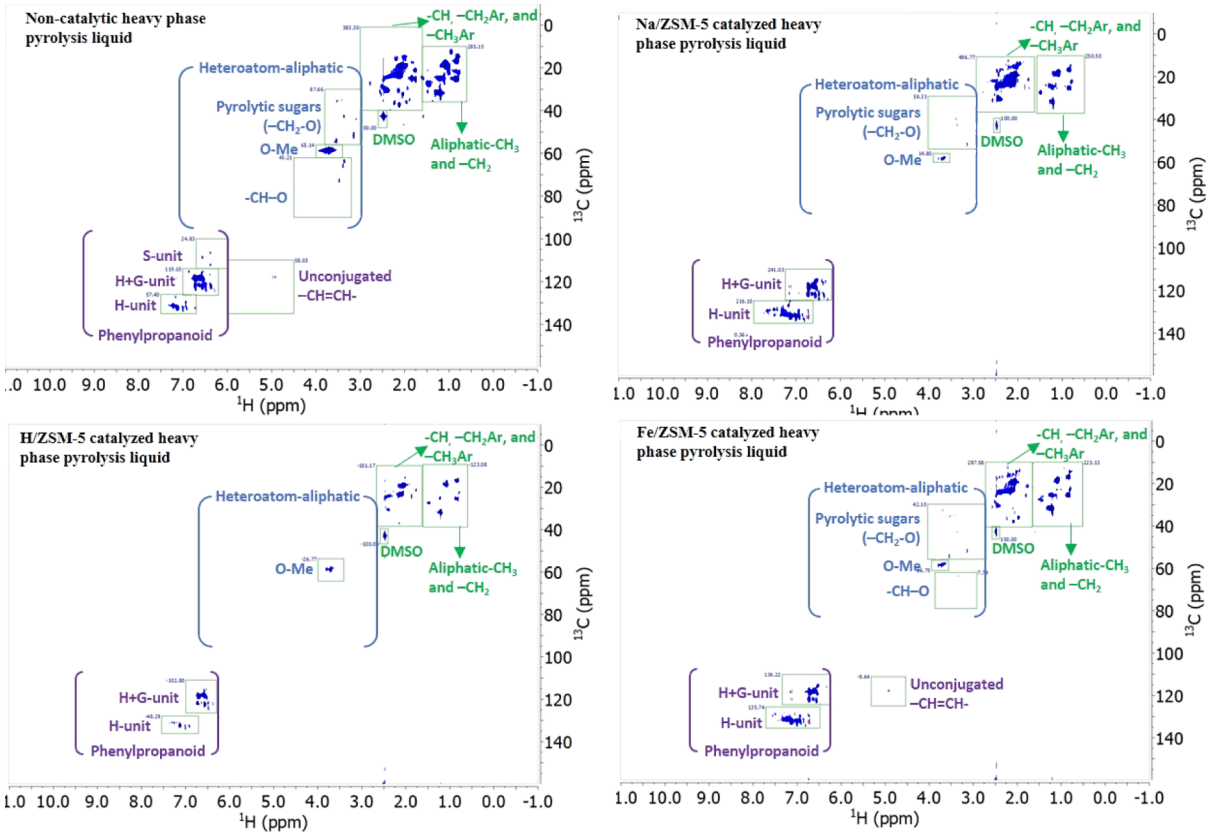

Figure 7. 2D-HSQC NMR comparison of heavy phase pyrolysis liquids produced by different catalysts.

https://dx.doi.org/10.1021/acs.energyfuels.0c02390
Energy Fuels 2020, 34, 12710−12723

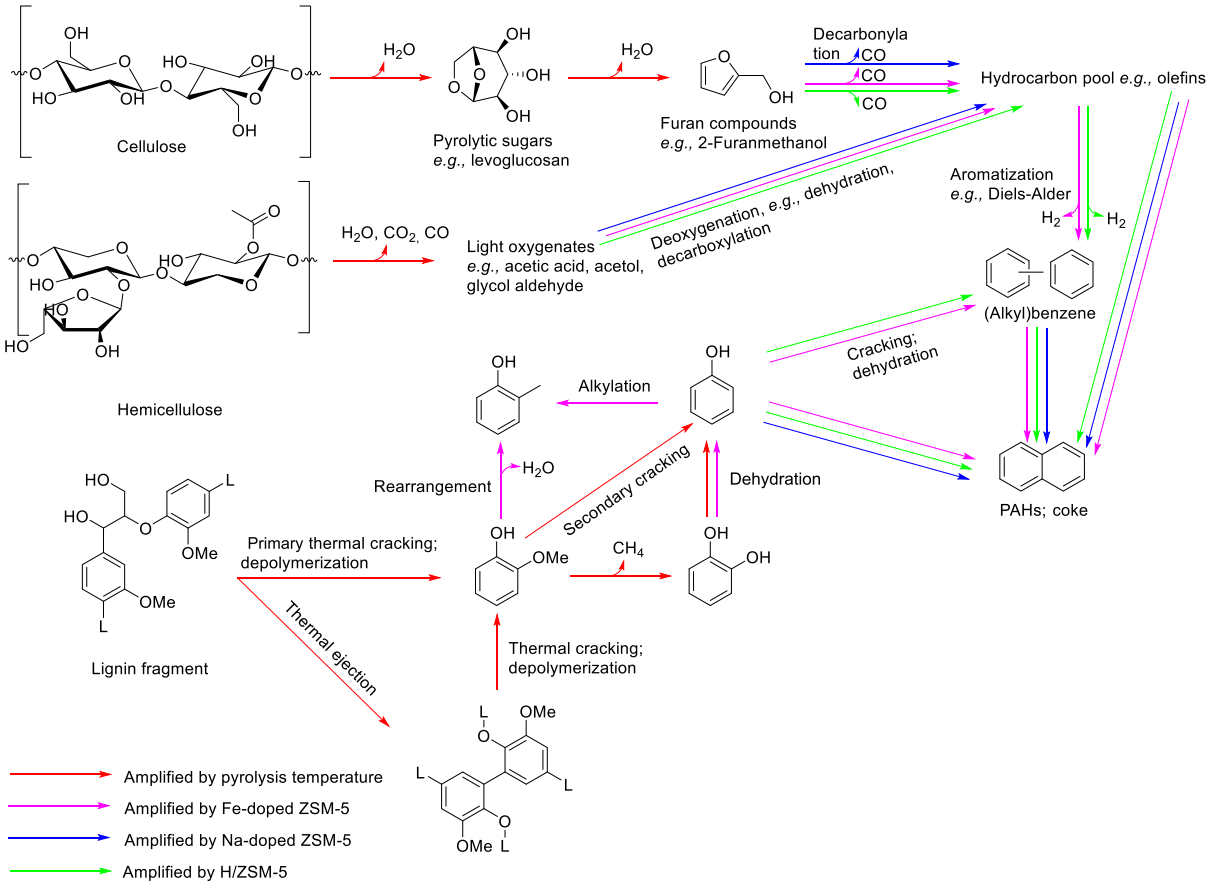

Figure 8. Proposed main reactions during fast pyrolysis and catalytic VPU of the feedstock.

partial thermochemical conversion reactions (*e.g.*, deoxygenations and demethoxylation) occurred, indicating that not all the chemical reactants in the vapor were converted. The reactions might have been limited by catalyst−vapor contact time, catalyst deactivation (*e.g.*, via coking or poisoning), and inadequate reactants from preceding reactions.

3.4. Reaction Pathways. Based on the analysis of the heavy phase catalytic VPU liquids, the main reaction pathways taking place during the process could be derived. The proposed pathway (Figure 8) assumes that the main components in the feedstock were lignin and residues of hemicellulose and cellulose. The arrows indicate which reactions are amplified by a certain catalyst; the absence of a reaction arrow does not necessarily imply that the reaction does not occur.

The red arrows indicate reactions that are favored by increasing temperature.[2] The blue arrows indicate reactions that are enhanced by metal-doped catalysts, and the green arrows indicate reactions that are catalyzed by H/ZSM-5. During fast pyrolysis, the cellulose and hemicellulose fractions are decomposed into pyrolytic sugars (*e.g.*, levoglucosan) by dehydration reactions and into light oxygenates (*e.g.*, carboxylic acids, ketones, and aldehydes) by ring scission and rearrangement reactions. Pyrolysis sugars further underwent dehydration and decarboxylation reactions forming furan compounds. These reactions were positively influenced by increasing fast pyrolysis temperature.

During catalytic VPU over metal-doped ZSM-5, furan compounds were decarbonylated into hydrocarbons (*e.g.*, olefins) and NCG.[59] Light oxygenates also undergo a deoxygenation reaction over H/ZSM-5 and metal-doped ZSM-5, producing hydrocarbons and water as a side product.[60] The formation pathway of aromatics (*e.g.*, monoaromatic hydrocarbons and polyaromatic hydrocarbons—MAHs and PAHs) occurs by Diels−Alder reactions of small, unsaturated hydrocarbons (hydrocarbon pool), potentially in combination with furans (i.e., Diels−Alder reaction with hydrocarbons followed by decarbonylation).[60,61]

Upon lignin fast pyrolysis, thermal ejection occurs (*e.g.*, phenolic dimers)[62,63] and primary depolymerization of lignin fragments and ejected aerosols results in substituted phenols that can undergo successive cracking and rearrangement reactions to yield phenol, catechol, and methylphenol. The latter methylphenol production is facilitated by the metal-doped zeolites, which is especially true for Fe/ZSM-5 when compared to Na/ZSM-5 as indicated in the scheme. In the presence of metal-doped ZSM-5 catalysts, demethylation reactions are thus enhanced, which also produces catechol and methyl-substituted ring products (*e.g.*, toluene and cresol).[64] Catechol may further react to phenolics and alcohol groups (*e.g.*, methanol) *via* a demethoxylation reaction.[65] High quantities in alkylphenols can also be due to alkylation of phenol.[54]

The conversion of phenolics into aromatics according to the results obtained in this study could occur via two reaction pathways. In the presence of the H/ZSM-5 catalyst, phenolics convert into PAHs and MAHs via aromatic-based cycle reactions.[60] In such cycle, phenol and other oxygenates can convert to methylbenzenes, which in turn forms MAH and olefins. The second pathway is the combination of

https://dx.doi.org/10.1021/acs.energyfuels.0c02390
Energy Fuels 2020, 34, 12710−12723

deoxygenation and decarboxylation reactions producing MAH, water, and NCG, followed by aromatization reactions into PAH and hydrogen gas in the presence of Na/ZSM-5 and Fe/ZSM-5 catalysts.[60] A higher selectivity of Fe/ZSM-5 (as opposed to Na/ZSM-5) toward monoaromatics rather than PAH was not observed in this study and hence not annotated in the proposed reaction pathway scheme.[45]

4. CONCLUSIONS

This work outlines the (i) results from LRDS analysis, (ii) yields from lab-scale (60 g per hour) fast pyrolysis with different VPU catalysts for lignin vapors, and (iii) comprehensive characterization of resulting products, a relatively unique feature to the current literature. Catalytic VPU with staged condensation of LRDS over H/ZSM-5, Na/ZSM-5, and Fe/ZSM-5 catalysts yielded heavy phase pyrolysis liquids in the range of 8.7−9.8 wt %. This is half of the heavy phase quantity obtained for noncatalytic pyrolysis of the same feedstock. However, all three ZSM-5 catalysts produced higher quality pyrolysis liquids by means of their volatile fraction size, aromatic contents, and alkylphenolic contents, if compared to their noncatalytic counterparts, albeit at lower overall C yields. The volatile fraction of the heavy phase was higher (21.6−33.1 wt % compared to 16.1 wt % for the case of noncatalytic pyrolysis). The heavy phase was enriched in valuable alkylphenols (12.0−15.9 wt %, compared to 1.5 wt %, on liquid basis) and aromatics (2.3−4.9 wt % compared to 0.6 wt % pyrolysis liquid basis). The heavy phase yield and its chemical composition also differed depending on the catalyst dopants, of which Fe/ZSM-5 was most favorable in terms of absolute alkylphenol yield. H/ZSM-5 showed the highest yield in heavy phase, Na/ZSM-5 produced the lowest oxygen mass fraction, and Fe/ZSM-5 produced the highest fraction of low-molecular-weight chemical compounds, like alkylphenols, being of interest for chemical recovery (*i.e.*, as fuel additives). Additionally, the catalytic processing in lignin pyrolysis yields more deoxygenated liquids, with less-reactive oxygenates and enriched in aromatics, which makes the liquid pyrolysis products more suitable for cofeeding in the existing petrorefineries.

AUTHOR INFORMATION

Corresponding Authors

Neil Priharto − *School of Life Sciences and Technology, Institut Teknologi Bandung, Bandung 40132, Indonesia; Department of Green Chemistry & Technology, Ghent University, Gent 9000, Belgium*; Email: Neil.Priharto@UGent.be

Stef Ghysels − *Department of Green Chemistry & Technology, Ghent University, Gent 9000, Belgium*; orcid.org/0000-0002-6957-725X; Email: Stef.Ghysels@UGent.be

Frederik Ronsse − *Department of Green Chemistry & Technology, Ghent University, Gent 9000, Belgium*; orcid.org/0000-0002-3290-9177; Email: Frederik.Ronsse@UGent.be

Wolter Prins − *Department of Green Chemistry & Technology, Ghent University, Gent 9000, Belgium*; Email: wolter.Prins@ugent.be

Authors

Mehmet Pala − *Department of Green Chemistry & Technology, Ghent University, Gent 9000, Belgium*

Wim Opsomer − *Department of Green Chemistry & Technology, Ghent University, Gent 9000, Belgium*

Güray Yildiz − *Department of Energy Systems Engineering, Izmir Institute of Technology, Urla 35430, Izmir, Turkey*; orcid.org/0000-0001-7399-0605

Hero Jan Heeres − *Department of Chemical Engineering, University of Groningen, AG Groningen 9747, The Netherlands*; orcid.org/0000-0002-1249-543X

Peter J. Deuss − *Department of Chemical Engineering, University of Groningen, AG Groningen 9747, The Netherlands*; orcid.org/0000-0002-2254-2500

Complete contact information is available at: https://pubs.acs.org/10.1021/acs.energyfuels.0c02390

Author Contributions

The manuscript was written through contributions of all authors. All authors have given approval to the final version of the manuscript.

Notes

The authors declare no competing financial interest.

ACKNOWLEDGMENTS

The authors would like to acknowledge the following colleagues and organization for their significant contribution: Prof. Bartel Vanholme from the VIB Department of Plant Systems Biology for his assistance in Klason lignin analyses; Léon Rohrbach from the Faculty of Mathematics and Natural Sciences, Chemical Technology Engineering and Technology Institute, University of Groningen, for his assistance in TGA, ICP-OES, and GC × GCMS analyses; and Dr. P.J. (Peter) Deuss for his assistance in 2D HSQC NMR analysis and data interpretation. The Multidisciplinary Research Platform "Ghent Bio-economy" is acknowledged for providing access to the lignin feedstock. The LOTUS Programme of the European Union is acknowledged for providing a doctoral scholarship.

ABBREVIATIONS AND SYMBOLS

a.r. = as received
CFP = catalytic fast pyrolysis
COD = chemical oxygen demand
daf = dry and ash free
d.b. = dry basis
DW = dry weight
ESP = electrostatic precipitator
LRDS = lignin-rich digested stillage
LOI = loss on ignition
HRT = hydraulic retention time
NCG = non-condensable gases
OLR = organic loading rate
VPU = vapor-phase upgrading
A_c = ash content of char (wt %)
$m_{aq,h}$ = amount of aqueous phase in ESP (g)
m_{co} = amount of char in heavy phase (g)
$m_{cond,i}$; $m_{cond,f}$ = weight difference of condenser flasks before and after experiment (g)
$m_{c,rm}$ = amount of char that was taken for analysis sample (g)
m_f = feedstock mass (g)
$m_{filter,i}$; $m_{filter,f}$ = weight difference of cotton filter before and after experiment (g)
$m_{h,aq}$ = amount of heavy phase in condenser flasks (g)
$m_{ESP,i}$; $m_{ESP,f}$ = weight difference of cotton filter before and after experiment (g)

$\overline{Q_b}$ = average baseline volumetric gas flow (L h^{-1})
$\overline{Q_s}$ = average volumetric gas flow during feeding (L h^{-1})
t = experiment time (h)
ω_C = mass fraction of carbon (wt %)
ω_H = mass fraction of hydrogen (wt %)
ω_N = mass fraction of nitrogen (wt %)
ω_O = mass fraction of oxygen (wt %)
Y_{aq} = aqueous phase pyrolysis liquids yield (wt %)
Y_c = char yield (wt %)
Y_{heavy} = heavy phase pyrolysis liquids yield (wt %)
Y_{NCG} = NCG yield (wt %)
Y_{tot} = total yield (wt %)
Δm_{loi} = weight difference of sand/char mixture on LOI testing (g)
ρ_{NCG} = gas density at gas outlet temperature (g L^{-1})

REFERENCES

(1) Ghysels, S.; Ronsse, F.; Dickinson, D.; Prins, W. Production and characterization of slow pyrolysis biochar from lignin-rich digested stillage from lignocellulosic ethanol production. *Biomass Bioenergy* **2019**, *122*, 349−360.
(2) Priharto, N.; Ronsse, F.; Yildiz, G.; Heeres, H. J.; Deuss, P. J.; Prins, W. Fast pyrolysis with fractional condensation of lignin-rich digested stillage from second-generation bioethanol production. *J. Anal. Appl. Pyrolysis* **2020**, *145*, 104756.
(3) Nowakowski, D. J.; Bridgwater, A. V.; Elliott, D. C.; Meier, D.; de Wild, P. Lignin fast pyrolysis: Results from an international collaboration. *J. Anal. Appl. Pyrolysis* **2010**, *88*, 53−72.
(4) Bridgwater, A. V. Review of fast pyrolysis of biomass and product upgrading. *Biomass Bioenergy* **2012**, *38*, 68−94.
(5) Bridgwater, A. V.; Meier, D.; Radlein, D. An overview of fast pyrolysis of biomass. *Org. Geochem.* **1999**, *30*, 1479−1493.
(6) Li, C.; Zhao, X.; Wang, A.; Huber, G. W.; Zhang, T. Catalytic Transformation of Lignin for the Production of Chemicals and Fuels. *Chem. Rev.* **2015**, *115*, 11559−11624.
(7) Ben, H.; Wu, F.; Wu, Z.; Han, G.; Jiang, W.; Ragauskas, A. J. A comprehensive characterization of pyrolysis oil from softwood barks. *Polymers* **2019**, *11*, 1387.
(8) Fahmi, R.; Bridgwater, A. V.; Donnison, I.; Yates, N.; Jones, J. M. The effect of lignin and inorganic species in biomass on pyrolysis oil yields, quality and stability. *Fuel* **2008**, *87*, 1230−1240.
(9) Lyckeskog, H. N.; Mattsson, C.; Olausson, L.; Andersson, S.-I.; Vamling, L.; Theliander, H. Thermal stability of low and high Mw fractions of bio-oil derived from lignin conversion in subcritical water. *Biomass Convers. Biorefin.* **2017**, *7*, 401−414.
(10) Zhou, S.; Garcia-Perez, M.; Pecha, B.; Kersten, S. R. A.; McDonald, A. G.; Westerhof, R. J. M. Effect of the fast pyrolysis temperature on the primary and secondary products of lignin. *Energy Fuels* **2013**, *27*, 5867−5877.
(11) Brown, T. R.; Thilakaratne, R.; Brown, R. C.; Hu, G. Techno-economic analysis of biomass to transportation fuels and electricity via fast pyrolysis and hydroprocessing. *Fuel* **2013**, *106*, 463−469.
(12) Venderbosch, R. H.; Ardiyanti, A. R.; Wildschut, J.; Oasmaa, A.; Heeres, H. J. Stabilization of biomass-derived pyrolysis oils. *J. Chem. Technol. Biotechnol.* **2010**, *85*, 674−686.
(13) Kloekhorst, A.; Wildschut, J.; Heeres, H. J. Catalytic hydrotreatment of pyrolytic lignins to give alkylphenolics and aromatics using a supported Ru catalyst. *Catal. Sci. Technol.* **2014**, *4*, 2367−2377.
(14) Meier, D.; Van De Beld, B.; Bridgwater, A. V.; Elliott, D. C.; Oasmaa, A.; Preto, F. State-of-the-art of fast pyrolysis in IEA bioenergy member countries. *Renewable Sustainable Energy Rev.* **2013**, *20*, 619−641.
(15) Zhang, L.; Liu, R.; Yin, R.; Mei, Y. Upgrading of bio-oil from biomass fast pyrolysis in China: A review. *Renewable Sustainable Energy Rev.* **2013**, *24*, 66−72.
(16) Kloekhorst, A.; Heeres, H. J. Catalytic Hydrotreatment of Alcell Lignin Using Supported Ru, Pd, and Cu Catalysts. *ACS Sustainable Chem. Eng.* **2015**, *3*, 1905−1914.
(17) Venderbosch, R. H. A critical view on catalytic pyrolysis of biomass. *ChemSusChem* **2015**, *8*, 1306−1316.
(18) Paasikallio, V.; Lindfors, C.; Kuoppala, E.; Solantausta, Y.; Oasmaa, A.; Lehto, J.; Lehtonen, J. Product quality and catalyst deactivation in a four day catalytic fast pyrolysis production run. *Green Chem.* **2014**, *16*, 3549−3559.
(19) Zhou, L.; Jia, Y.; Nguyen, T.-H.; Adesina, A. A.; Liu, Z. Hydropyrolysis characteristics and kinetics of potassium-impregnated pine wood. *Fuel Process. Technol.* **2013**, *116*, 149−157.
(20) Asadieraghi, M.; Wan Daud, W. M. A. In-situ catalytic upgrading of biomass pyrolysis vapor: Co-feeding with methanol in a multi-zone fixed bed reactor. *Energy Convers. Manage.* **2015**, *92*, 448−458.
(21) Yildiz, G.; Ronsse, F.; Vercruysse, J.; Daels, J.; Toraman, H. E.; Van Geem, K. M.; Marin, G. B.; Van Duren, R.; Prins, W. In situ performance of various metal doped catalysts in micro-pyrolysis and continuous fast pyrolysis. *Fuel Process. Technol.* **2016**, *144*, 312−322.
(22) Biddy, M., Dutta, A. *Ex Situ Catalytic Fast Pyrolysis Technology Pathway Ex Situ Catalytic Fast Pyrolysis Technology Pathway NREL/TP-51*; NREL, 2013.
(23) Engtrakul, C.; Mukarakate, C.; Starace, A. K.; Magrini, K. A.; Rogers, A. K.; Yung, M. M. Effect of ZSM-5 acidity on aromatic product selectivity during upgrading of pine pyrolysis vapors. *Catal. Today* **2016**, *269*, 175−181.
(24) Yung, M. M.; Starace, A. K.; Mukarakate, C.; Crow, A. M.; Leshnov, M. A.; Magrini, K. A. Biomass Catalytic Pyrolysis on Ni/ZSM-5: Effects of Nickel Pretreatment and Loading. *Energy Fuels* **2016**, *30*, 5259−5268.
(25) Grams, J.; Ruppert, A. Development of heterogeneous catalysts for thermo-chemical conversion of lignocellulosic biomass. *Energies* **2017**, *10*, 545.
(26) Liang, J.; Morgan, H. M.; Liu, Y.; Shi, A.; Lei, H.; Mao, H.; Bu, Q. Enhancement of bio-oil yield and selectivity and kinetic study of catalytic pyrolysis of rice straw over transition metal modified ZSM-5 catalyst. *J. Anal. Appl. Pyrolysis* **2017**, *128*, 324−334.
(27) Ben, H.; Ragauskas, A. J. Influence of Si / Al Ratio of ZSM-5 Zeolite on the Properties of Lignin Pyrolysis Products. *ACS Sustainable Chem. Eng.* **2013**, *1*, 316−324.
(28) Jiang, X.; Su, X.; Bai, X.; Li, Y.; Yang, L.; Zhang, K.; Zhang, Y.; Liu, Y.; Wu, W. Conversion of methanol to light olefins over nanosized [Fe,Al]ZSM-5 zeolites: Influence of Fe incorporated into the framework on the acidity and catalytic performance. *Microporous Mesoporous Mater.* **2018**, *263*, 243−250.
(29) Xu, L.; Yao, Q.; Zhang, Y.; Fu, Y. Integrated Production of Aromatic Amines and N-Doped Carbon from Lignin via ex Situ Catalytic Fast Pyrolysis in the Presence of Ammonia over Zeolites. *ACS Sustainable Chem. Eng.* **2017**, *5*, 2960−2969.
(30) Duan, D.; Wang, Y.; Dai, L.; Ruan, R.; Zhao, Y.; Fan, L.; Tayier, M.; Liu, Y. Ex-situ catalytic co-pyrolysis of lignin and polypropylene to upgrade bio-oil quality by microwave heating. *Bioresour. Technol.* **2017**, *241*, 207−213.
(31) Ryu, S.; Lee, H. W.; Kim, Y.-M.; Jae, J.; Jung, S.-C.; Ha, J.-M.; Park, Y.-K. Catalytic fast co-pyrolysis of organosolv lignin and polypropylene over in-situ red mud and ex-situ HZSM-5 in two-step catalytic micro reactor. *Appl. Surf. Sci.* **2020**, *511*, 145521.
(32) Mullen, C. A.; Boateng, A. A. Catalytic pyrolysis-GC/MS of lignin from several sources. *Fuel Process. Technol.* **2010**, *91*, 1446−1458.
(33) Kim, B.-S.; Jeong, C. S.; Kim, J. M.; Park, S. B.; Park, S. H.; Jeon, J.-K.; Jung, S.-C.; Kim, S. C.; Park, Y.-K. Ex situ catalytic upgrading of lignocellulosic biomass components over vanadium contained H-MCM-41 catalysts. *Catal. Today* **2016**, *265*, 184−191.
(34) Ghysels, S.; Dubuisson, B.; Pala, M.; Rohrbach, L.; Van den Bulcke, J.; Heeres, H. J.; Ronsse, F. Improving fast pyrolysis of lignin using three additives with different modes of action. *Green Chem.* **2020**, DOI: 10.1039/D0GC02417A. , accepted manuscript

https://dx.doi.org/10.1021/acs.energyfuels.0c02390
Energy Fuels 2020, 34, 12710−12723

(35) Zhang, S.; Yang, M.; Shao, J.; Yang, H.; Zeng, K.; Chen, Y.; Luo, J.; Agblevor, F. A.; Chen, H. The conversion of biomass to light olefins on Fe-modified ZSM-5 catalyst: Effect of pyrolysis parameters. *Sci. Total Environ.* **2018**, *628−629*, 350−357.
(36) Xie, W.; Liang, J.; Morgan, H. M., Jr.; Zhang, X.; Wang, K.; Mao, H.; Bu, Q. Ex-situ catalytic microwave pyrolysis of lignin over Co/ZSM-5 to upgrade bio-oil. *J. Anal. Appl. Pyrolysis* **2018**, *132*, 163−170.
(37) Zhou, G.; Jensen, P. A.; Le, D. M.; Knudsen, N. O.; Jensen, A. D. Direct upgrading of fast pyrolysis lignin vapor over the HZSM-5 catalyst. *Green Chem.* **2016**, *18*, 1965−1975.
(38) Lee, H. W.; Kim, Y.-M.; Jae, J.; Sung, B. H.; Jung, S.-C.; Kim, S. C.; Jeon, J.-K.; Park, Y.-K. Catalytic pyrolysis of lignin using a two-stage fixed bed reactor comprised of in-situ natural zeolite and ex-situ HZSM-5. *J. Anal. Appl. Pyrolysis* **2016**, *122*, 282−288.
(39) Zhao, Y.; Deng, L.; Liao, B.; Fu, Y.; Guo, Q.-X. Aromatics Production via Catalytic Pyrolysis of Pyrolytic Lignins from Bio-Oil. *Energy Fuels* **2010**, *24*, 5735−5740.
(40) Fan, L.; Chen, P.; Zhou, N.; Liu, S.; Zhang, Y.; Liu, Y.; Wang, Y.; Omar, M. M.; Peng, P.; Addy, M.; Cheng, Y.; Ruan, R. In-situ and ex-situ catalytic upgrading of vapors from microwave-assisted pyrolysis of lignin. *Bioresour. Technol.* **2018**, *247*, 851−858.
(41) Ghysels, S.; Acosta, N.; Estrada, A.; Pala, M.; De Vrieze, J.; Ronsse, F.; Rabaey, K. Integrating anaerobic digestion and slow pyrolysis improves the product portfolio of a cocoa waste biorefinery. *Sustainable Energy Fuels* **2020**, *4*, 3712−3725.
(42) Imran, A.; Bramer, E.; Seshan, K.; Brem, G. Catalytic flash pyrolysis of biomass using different types of zeolites and online vapor fractionation. *Energies* **2016**, *9*, 187.
(43) Zhang, B.; Zhong, Z.-P.; Wang, X.-B.; Ding, K.; Song, Z.-W. Catalytic upgrading of fast pyrolysis biomass vapors over fresh, spent and regenerated ZSM-5 zeolites. *Fuel Process. Technol.* **2015**, *138*, 430−434.
(44) López-Renau, L. M.; García-Pina, L.; Hernando, H.; Gómez-Pozuelo, G.; Botas, J. A.; Serrano, D. P. Enhanced bio-oil upgrading in biomass catalytic pyrolysis using KH-ZSM-5 zeolite with acid-base properties. *Biomass Convers. Biorefin.* **2019**, *302*, 1.
(45) Sun, L.; Zhang, X.; Chen, L.; Zhao, B.; Yang, S.; Xie, X. Comparision of catalytic fast pyrolysis of biomass to aromatic hydrocarbons over ZSM-5 and Fe/ZSM-5 catalysts. *J. Anal. Appl. Pyrolysis* **2016**, *121*, 342−346.
(46) Amdebrhan, B. T. Evaluating the Performance of Activated Carbons, Polymeric and Zeolite Adsorbents for Volatile Organic Compounds Control. MSc Dissertation, University of Alberta, Canada, 2018, p 125.
(47) Yildiz, G.; Lathouwers, T.; Toraman, H. E.; Van Geem, K. M.; Marin, G. B.; Ronsse, F.; Van Duren, R.; Kersten, S. R. A.; Prins, W. Catalytic fast pyrolysis of pine wood: Effect of successive catalyst regeneration. *Energy Fuels* **2014**, *28*, 4560−4572.
(48) Domalski, E. S.; Jobe, T. L., Jr.; Milne, T. A. Thermodynamic data for biomass conversion and waste incineration. National Bureau of Standards: Washington, DC (US), 1986 p 350.
(49) Yin, W.; Venderbosch, R. H.; Bottari, G.; Krawzcyk, K. K.; Barta, K.; Heeres, H. J. Catalytic upgrading of sugar fractions from pyrolysis oils in supercritical mono-alcohols over Cu doped porous metal oxide. *Appl. Catal., B* **2015**, *166−167*, 56−65.
(50) Wildschut, J.; Mahfud, F. H.; Venderbosch, R. H.; Heeres, H. J. Hydrotreatment of Fast Pyrolysis Oil Using Heterogeneous Noble-Metal Catalysts. *Ind. Eng. Chem. Res.* **2009**, *48*, 10324−10334.
(51) Lancefield, C. S.; Panovic, I.; Deuss, P. J.; Barta, K.; Westwood, N. J. Pre-treatment of lignocellulosic feedstocks using biorenewable alcohols: towards complete biomass valorisation. *Green Chem.* **2017**, *19*, 202−214.
(52) Carlson, T. R.; Jae, J.; Lin, Y.-C.; Tompsett, G. A.; Huber, G. W. Catalytic fast pyrolysis of glucose with H/ZSM-5: The combined homogeneous and heterogeneous reactions. *J. Catal.* **2010**, *270*, 110−124.
(53) Li, P.; Li, D.; Yang, H.; Wang, X.; Chen, H. Effects of Fe-, Zr-, and Co-Modified Zeolites and Pretreatments on Catalytic Upgrading of Biomass Fast Pyrolysis Vapors. *Energy Fuels* **2016**, *30*, 3004−3013.
(54) Xu, W.; Miller, S. J.; Agrawal, P. K.; Jones, C. W. Zeolite topology effects in the alkylation of phenol with propylene. *Appl. Catal., A* **2013**, *459*, 114−120.
(55) Helmut, F. Cresols and Xylenols. *Ullmann's Encyclopedia of Industrial Chemistry*, 2012; Vol. *10*, pp 673−710.
(56) Zhang, H.; Zheng, J.; Xiao, R. Catalytic pyrolysis of willow wood with Me/ZSM-5 (Me = Mg, K, Fe, Ga, Ni) to produce aromatics and olefins. *BioResources* **2013**, *8*, 5612−5621.
(57) Mullen, C. A.; Boateng, A. A. Production of Aromatic Hydrocarbons via Catalytic Pyrolysis of Biomass over Fe-Modified H/ZSM-5 Zeolites. *ACS Sustainable Chem. Eng.* **2015**, *3*, 1623−1631.
(58) Wąchaw, A.; Nowińska, K.; Schwieger, W. Benzene to phenol oxidation over iron exchanged zeolite ZSM-5. *Appl. Catal., A* **2004**, *270*, 151−156.
(59) Moldoveanu, S. C. Chapter 19 Pyrolysis of Various Derivatives of Carboxylic Acids. *Tech. Instrum. Anal. Chem.* **2010**, *28*, 579−627.
(60) Wang, K.; Johnston, P. A.; Brown, R. C. Comparison of in-situ and ex-situ catalytic pyrolysis in a micro-reactor system. *Bioresour. Technol.* **2014**, *173*, 124−131.
(61) Mullen, C. A.; Tarves, P. C.; Raymundo, L. M.; Schultz, E. L.; Boateng, A. A.; Trierweiler, J. O. Fluidized Bed Catalytic Pyrolysis of Eucalyptus over H/ZSM-5: Effect of Acid Density and Gallium Modification on Catalyst Deactivation. *Energy Fuels* **2018**, *32*, 1771−1778.
(62) Bai, X.; Kim, K. H.; Brown, R. C.; Dalluge, E.; Hutchinson, C.; Lee, Y. J.; Dalluge, D. Formation of phenolic oligomers during fast pyrolysis of lignin. *Fuel* **2014**, *128*, 170−179.
(63) Piskorz, J., Majerski, P., Radlein, D. Pyrolysis of Biomass—Aerosol Generation: Properties, Applications, and Significance for Process Engineers. *Biomass, A Growth Opportunity in Green Energy and Value-Added Products; 4th Biomass Conference of the Americas*, 1999; pp 1153−1159.
(64) Peters, J. E.; Carpenter, J. R.; Dayton, D. C. Anisole and Guaiacol Hydrodeoxygenation Reaction Pathways over Selected Catalysts. *Energy Fuels* **2015**, *29*, 909−916.
(65) Ishikawa, M.; Tamura, M.; Nakagawa, Y.; Tomishige, K. Demethoxylation of guaiacol and methoxybenzenes over carbon-supported Ru-Mn catalyst. *Appl. Catal., B* **2016**, *182*, 193−203.

https://dx.doi.org/10.1021/acs.energyfuels.0c02390
Energy Fuels 2020, 34, 12710−12723